

Focus On What’s Important: Self-Attention Model for Human Pose Estimation

Guanxiong Sun, Chenqin Ye, and Kuanquan Wang

Harbin Institute of Technology, Harbin 150001, China
wangkq@hit.edu.cn

Abstract. Human pose estimation is an essential yet challenging task in computer vision. One of the reasons for this difficulty is that there are many redundant regions in the images. In this work, we proposed a convolutional network architecture combined with the novel attention model. We named it attention convolutional neural network (ACNN). ACNN learns to focus on specific regions of different input features. It’s a multi-stage architecture. Early stages filtrate the “nothing-regions”, such as background and redundant body parts. And then, they submit the important regions which contain the joints of the human body to the following stages to get a more accurate result. What’s more, it doesn’t require extra manual annotations and self-learning is one of our intentions. We separately trained the network because the attention learning task and the pose estimation task are not independent. State-of-the-art performance is obtained on the MPII benchmarks.

Keywords: Human Pose Estimation, Attention Model.

1 Introduction

Human pose estimation means locating the body joints for human in a given picture. It serves as the basis for higher level computer vision tasks, e.g., human activity recognition [1, 2], human computer interaction and cloth parsing [3, 4]. However, getting accurate locations is still challenging because of the articulation of body limbs, self-occlusion, various clothing, and foreshortening.

Recently, lots of methods based on deep convolutional neural networks (CNNs) have made great progress in almost every field of computer vision. As for human pose estimation, there are also many different methods [5, 6, 7, 8, 9]. In these methods, CNNs take a set of images as input, firstly extract features using kinds of different architectures such as VGGs [10], Inception models [11, 12, 13] and ResNets [14], then several layers are applied to get the prediction result (heatmap). A representative pipeline and an example of a set of heatmaps are shown in Fig. 1. In these models, CNNs have to handle entire regions of the input images, which goes against with human beings. As shown on the right side of the input image in Fig. 1, there are many redundant parts of human body which would confuse network to predict accurate locations. More broadly the background regions that almost exist in every image are

worthless to our task. These regions should be filtered out. Humans do not take account of every single pixel of an image. In other words, we merely need to focus on what's important to our goal. This mechanism is called visual attention scheme.

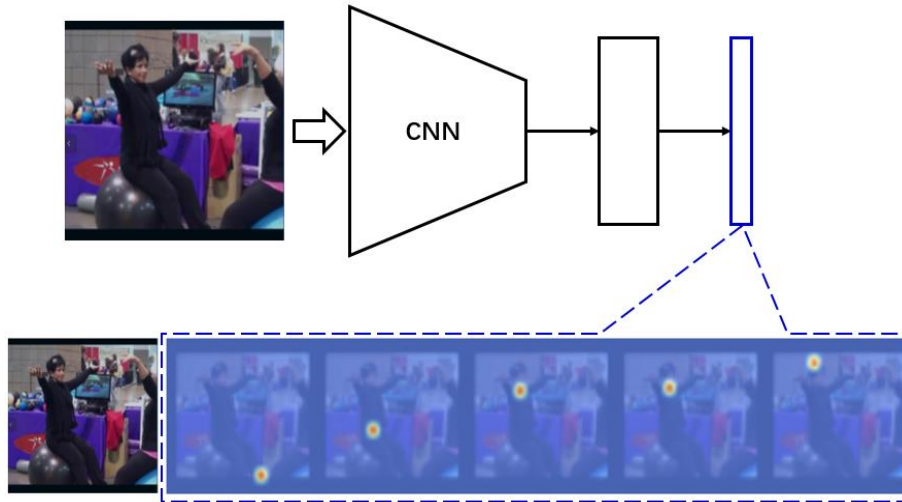


Fig. 1. Up: Traditional pipeline in pose estimation, CNN is used as a feature extractor. Then several convolution layers are connected to generate heatmap, which is represented by a box colored in blue. **Down:** Some samples of heatmap (produced by our model). On the right is the input image. On the left are heatmaps for different body joints.

In this work, we proposed an attention convolutional neural network (ACNN) architecture which integrates the attention model into the neural network. Hardly any method of human pose estimation has fused attention mechanism. Without kinds of extra manual annotations, we designed the network to learn the attention scheme itself, which depends on different input images. Our insight is shown in Fig. 2. The proposed ACNN is an end-to-end model based on the previous method stacked Hour-glass Network [15]. It's a multi-stage network, details in [15]. In our method, the procedure consists of two goals, attention learning and prediction learning. The attention network learns to generate a mask to represent the attention scheme, which aims to select important regions of the input features. Only the selected regions will be passed to the subsequent stages. The other network learns to predict the locations of human body joints. ACNN is also a multi-stage architecture. These heatmaps are not only generated by a single stage but also by the foregoing stages, because of the selection operated by attention masks. So that the final result is made of all intermediate stages. In this way our method can learn different attention on different stages, meanwhile it filters out “deceptive” regions, and gets a more accurate result from this refine procedure.

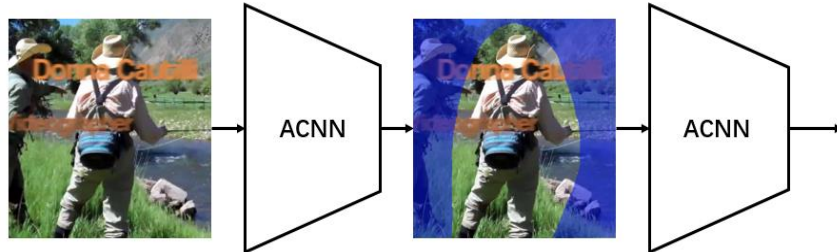


Fig. 2. Original images are firstly passed into ACNN. At the end of each stage, ACNN produces an attention mask, which is used to select important regions to pass into following stages. The blue regions are what filtered out by the previous stage’s attention mask. This helps networks more focus on regions that are informative and imperative.

We have done experiments on MPII Human Pose dataset to demonstrate the effectiveness of our attention model. Our approach improved the base architecture apparently and get the state-of-art results compared to all public methods on the benchmark. Our work can be summarized as follows:

- We propose an attention convolutional neural network (ACNN), in which attention scheme is simultaneously integrated to enhance the model’s ability to focus on important regions of input features.
- We conduct experiments on MPII dataset to demonstrate the effectiveness of ACNN, and we achieve superior performance over the state-of-the-art results.

2 Related Work

2.1 Human Pose Estimation

Before “DeepPose” by Toshev et al. [16], research on human pose estimation is mainly based on graph structures, e.g., Pictorial structures [17, 18, 19] and loopy structures [20, 21, 22]. Without CNNs, all these works were designed on top of manual hand-crafted features. Toshev et al. extract features through CNN, and then use their network to regress the x , y coordinates of human body joints, which is the first attempt on using CNNs on this task. Although it significantly enhanced the performance than ever before, the results were limited by the complexity of directly learning x , y coordinates from region based feature maps. To solve this problem, researchers turned to the heatmap, which is made by placing Gaussian peaks at every joint location. Plenty of methods were designed to regress the heatmap instead of the x , y coordinates, such as Tompson et al. [23], Newell et al. [15], Wei et al. [24].

Our method is built on the basis of stack Hourglass Networks [15]. The Hourglass Module is a conv-deconv or encoder-decoder structure. We stack several stages of Hourglass Module and fuse attention model into the base network. The overview is briefly presented in Fig. 2, and details are described in Section 3.

2.2 Visual Attention Model

Recently visual attention models have achieved huge success and have been used for a lot of computer vision tasks, e.g., machine translation [25] and image captioning [26] and object recognition [27, 23]. In these methods, attention model is usually learned from extra bounding box manual annotations. Generally, they use attention to get a region based result and improve the neural networks' efficiency.

In this work the attention model is combined with the CNN architecture. To our knowledge, seldom researchers have done this before. In addition, we do not require extra manual annotations to learn the attention scheme.

3 Approach

In this section, we will introduce the proposed attention convolutional neural network (ACNN) for human pose estimation. Firstly, we discuss about the base network, stacked Hourglass Network. Then, we focus on the design process of the attention model and the way it combines with CNN.

A brief architecture of the ACNN is shown in Fig. 3. We take a two stages network for example. In our experiments, two more stages are stacked in a similar way. At the end of each stage, the attention network selects important regions to pass into following stages.

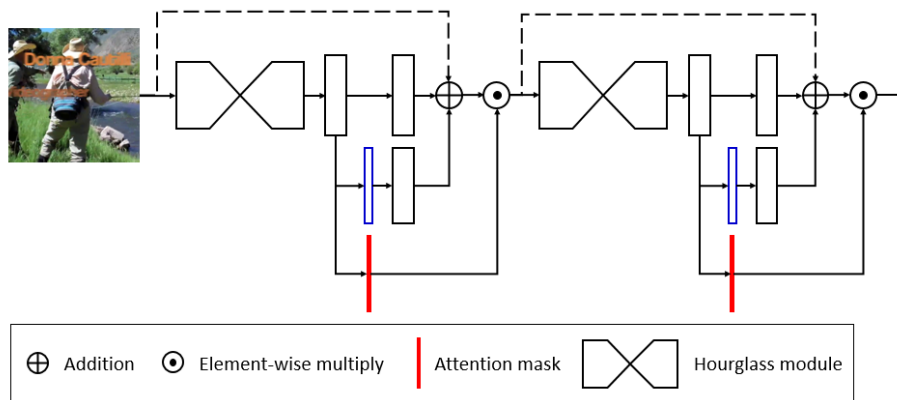


Fig. 3. Attention mask and heatmap are generated at the end of each stage. These attention masks are binary images whose size is the same as the input feature maps'. In our experiment, the size is 64×64 . Then we use an element-wise multiply to select informative and important regions of the feature maps to go through the rest of the architecture. The dotted lines indicate the Identity Mapping used in ResNet.

3.1 Base Network

Hourglass Network aims at capturing information at every scale in feed-forward structure. It first performs bottom-up processing by pooling, and conducts top-down

processing by upsampling. Feature maps at the same scale in this two procedures are then added together as the ResNet does. This bottom-up, top-down processing is repeated to build a “stacked hourglass” network, with intermediate supervision at the end of each stack.

We adopt a 4-stack hourglass network as the base network. The input images are 256×256 , and the output heatmaps are $K \times 64 \times 64$, where K is the number of human body joints. We follow previous works [15, 26] to use the Mean Squared Error as the criterion.

3.2 Attention Design

Our objective is to learn the attention scheme, which will help the network get the ability to decide where to “look”. It could be done easily if using manual annotations, for example, we can just let the network predict attention by regressing the bounding box like Fast R-CNN [28] or other detection methods [29, 30, 31] do. However, it’s a huge workload which is time-consuming and money-wasting. Moreover, it would not make any sense to the progress of deep learning by augment more labeled data. So we propose a reinforced method to make network learn the attention scheme itself.

ACNN also predicts attention at each stage, but it will not regress the bounding box regions. It will produce a binary mask, and the mask will then select the input feature maps to next stage, thus the predicted heatmap in the next stage is only on the selected regions. Then we add it with the regions of the previous heatmaps that are filtered out by the attention mask in the previous stage. In this way, the attention mask learning can be encoded in the pose estimation procedure which is shown in Fig. 3.

Inference. The full network starts with a 7×7 convolutional layer with stride 2, followed by a residual module and a round of max pooling to bring the resolution down from 256 to 64. Then several stacked hourglass modules are followed.

At the beginning of the procedure, we initialized the attention mask which defined as a binary image before with all ones Tensor to make all regions of input image pass into the network. At the end of the first stage, a new attention mask is generated by the first hourglass module along with the predicted heatmap. Then we use the new attention mask to select the input feature maps for the next stage. So the input feature maps of each stage can be formulated as,

$$X^{(i+1)} = f\left(\left(X^{(i)} + \theta\left(X^{(i)}; W^{(i)}\right)\right); \omega^{(i)}\right) \odot M^{(i)} \quad (1)$$

where $\theta(X^{(i)}; W^{(i)})$ denotes the transformation of the hourglass module which contains a series convolutional layers and pooling layers, details in [15]. $X^{(i)}$ denotes the input feature maps of the i -th stage. $f(\bullet)$ denotes the 1×1 convolutions after hourglass module. $M^{(i)}$ represents the attention mask produced by the i -th stage, which can be further decomposed as,

$$M^{(i)} = f_c\left(\left(X^{(i)} + \theta\left(X^{(i)}; W^{(i)}\right)\right); \omega^{(i)}\right) \quad (2)$$

where $f_c(\bullet)$ denotes the convolution layers to generate the binary masks.

During implementation, there is no kind of standard layer for a binary mask to filter out feature maps throughout all channels. In our experiments, since the input feature maps for every stage is a 256 channels' 3D tensor, we simply replicate the binary mask to the same channel number to the feature maps. And then perform an element-wise operation to select it. However, this could draw another problem in—gradient explosion. This is discussed in section 3.3.

We almost add Batch Normalization [35] and ReLU [32] at every convolutional layers to speed up the training process, except for the 1×1 convolutional layers to generate the heatmaps and the attention masks. We use sigmoid activation to generate the attention masks.

Loss Function. Once we use an attention mask to select regions. We can only get the results on the selected regions. Thus, we add the predicted heatmap with the discarded regions of the previous heatmaps. To illustrate more clearly, we use the word prediction to represent the final result of one stage. The prediction is not only associated with the heatmap produced by this stage. Because when compute the loss, computation should happen on all regions, but the heatmap is only on the selected regions by the previous attention mask. We must add the filtered out regions back to get an all-region prediction. For understanding, you may imagine each stage only generates the attention mask for the informative regions, so the discarded regions are redundant or simple regions, which are usually background. As a result, each stage only predicts the informative regions of the final prediction, and the simple regions are discarded by the previous stages. So we must add them together. This procedure is shown in Fig. 4

Then we can formulate the loss function as follow to train the network,

$$Loss = Mse(P; G) = \frac{1}{w \cdot h} \sum_{x=1}^w \sum_{y=1}^h (G_{x,y} - P_{x,y})^2 \quad (3)$$

where w, h indicate the width and height for the heatmaps, and G denotes the ground-truth. P denotes the final prediction of the model, which can be decomposed as,

$$P^{(i)} = H^{(i)} + P^{(i-1)} \odot \overline{M^{(i-1)}} \quad (4)$$

where $P^{(i)}$ is the produced prediction of the i -th stage. $H^{(i)}$ is the generated heatmap of the i -th stage, which is colored in blue in Fig. 4. $\overline{M^{(i-1)}}$ denotes the negation of $M^{(i-1)}$, the generated attention mask for the $(i-1)$ -th stage, which is colored in red in Fig. 4. And $M^{(i)}$ is decomposed in Eq.(2). So we can refine heatmaps and attention maps by this loss function.

When test, we obtain the final prediction from the heatmap generated by the last stack of hourglass by taking the locations with the maximum score as follows:

$$L_k = \arg \max_{m,n} P_k(m, n), \quad k = 1, \dots, K. \quad (5)$$

Where m, n denote the coordinate of every pixel on P , and k denotes the channel from 1 to K which is the total number of human body joints.

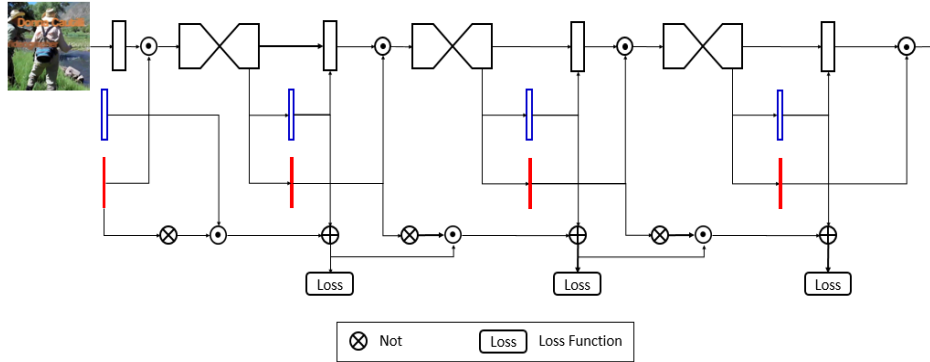


Fig. 4. The ACNN architecture added loss units for training. The prediction isn't just associated with the heatmap produced by this stage. The heatmap is only on the selected regions by the previous attention mask. We add the filtered out regions back to get an all-region prediction. We apply a Not operation to select the discarded regions of the previous heatmap and add it together with the new heatmap to get prediction result, and use it to compute the loss. Consequently, conduct back propagation.

3.3 Training Details

We evaluate our network on MPII Human Pose [27] benchmark datasets. MPII Human Pose consists of around 25k images with annotations for multiple people providing 40k annotated samples (28k training, 11k testing). Our implementation follows [15] using Torch. We use scaling, rotation, flipping to augment training dataset. We use RMSProp to optimize the network on 2 Titan X GPUs.

Multi-task Learning. Our model involves two kind of learning tasks. The first is predicting the heatmap for locating human body joints. The other one is learning the attention mask for selecting important regions. We separately trained our model mainly because these two tasks are not independent, not like the multi-task learning in Fast R-CNN [28].

We represent heatmap learning as task A and attention learning as task B. The result of task B has great influence on task A. For example, if task B filters out body regions, task A would never converge to a better solution, because the input feature maps do not contain much important information. Another reason is that the gradient problem caused by task B. The gradients for task B are much larger than those of task A. It happens due to the replication layers. That mean the gradient tensors of all channels are added back together to the attention mask's gradient tensor while executing back propagation.

So, firstly, we freeze the parameters of task B, and initialize all attention masks with all ones tensors. And we use a 4-stack architecture. We train task A with a mini-batch size of 12 (6 per GPU) for 200 epochs. The learning rate is initialized with 5×10^{-4} and is dropped by 10 at the 120th and the 170th epoch.

Then we freeze the parameters for task A, and train task B for another 200 epochs. The learning rate is initialized with 2.5×10^{-4} and is dropped by 10 at the 120th and the 170th epoch.

Finally, we jointly train the two tasks for 100 epochs. The learning rate is initialized with 2.5×10^{-4} and is dropped by 10 at the 50th and the 70th epoch.

4 Results

Evaluation. Evaluation is done using the standard Percentage of Correct Keypoints (PCK) [33] metric which reports the percentage of detections that fall within a normalized distance of the ground truth. For MPII, by a fraction of 50% of the head length (referred to as PCKh [27]).

MPII Human Pose. We achieve the state-of-the-art results on the MPII Human Pose dataset, which is shown in Table 1. Our approach is based on stacked Hourglass Networks [15]. Compare with [15], the precision of all joint parts are improved a lot. Specifically, our method improves the results on ankle by 2.3%. Example results can be seen in Fig. 5.

Table 1. Results on MPII Human Pose (PCKh@0.5)

Method	Head	Sho.	Elb.	Wri.	Hip	Kne.	Ank.	Total
Tompson et al. [34], CVPR'15	96.1	91.9	83.9	77.8	80.9	72.3	64.8	82.0
Pishchulin et al. [36], CVPR'16	94.1	90.2	83.4	77.3	82.6	75.7	68.6	82.4
Lifshitz et al. [37], ECCV'16	97.8	93.3	85.7	80.4	85.3	76.6	70.2	85.0
Gkioxary et al. [38], ECCV'16	96.2	93.1	86.7	82.1	85.2	81.4	74.1	86.1
Rafi et al. [39], BMVC'16	97.2	93.9	86.4	81.3	86.8	80.6	73.4	86.3
Wei et al. [24], CVPR'16	97.8	95.0	88.7	84.0	88.4	82.8	79.4	88.5
Insafutdinov et al [40]., ECCV'16	96.8	95.2	89.3	84.4	88.4	83.4	78.0	88.5
Newell et al. [15], ECCV'16	98.2	96.3	91.2	87.1	90.1	87.4	83.6	90.9
Luvizon et al. [41], arXiv'17	98.1	96.6	92.0	87.5	90.6	88.0	82.7	91.2
Ning et al. [42], TMM'17	98.1	96.3	92.2	87.8	90.6	87.6	82.7	91.2
Chu et al. [43], CVPR'17	98.5	96.3	91.9	88.1	90.6	88.0	85.0	91.5
Chou et al. [44], arXiv'17	98.2	96.8	92.2	88.0	91.3	89.1	84.9	91.8
Chen et al. [45], ICCV'17	98.1	96.5	92.5	88.5	90.2	89.6	86.0	91.9
Yang et al. [46], ICCV'17	98.5	96.7	92.5	88.7	91.1	88.6	86.0	92.0
Ours	98.5	96.4	92.5	88.5	91.6	88.9	85.9	92.0



Fig. 5. Example results on MPII human pose dataset

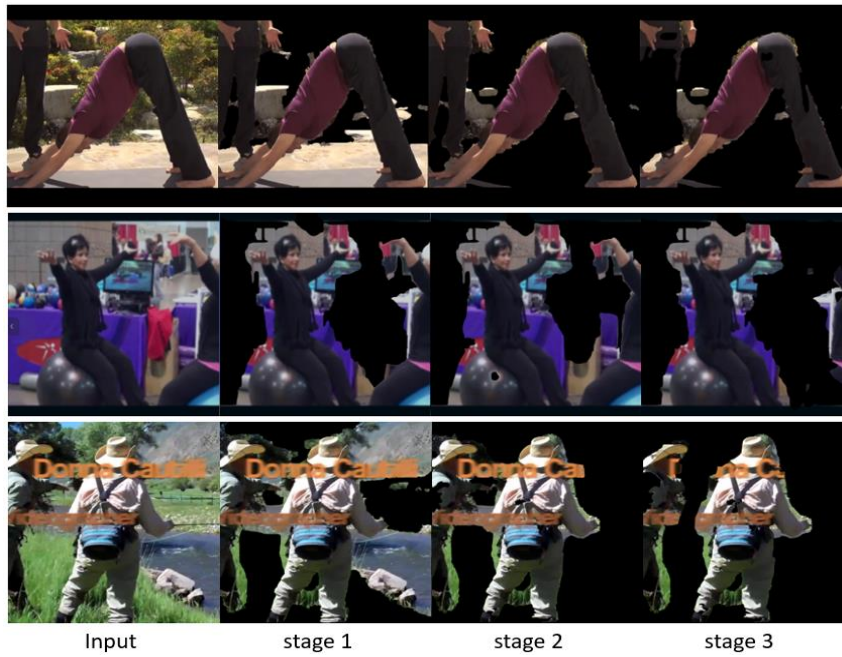


Fig. 6. The first column shows the input images, the rest column shows the attention map of different stage, the discarded regions are colored in black.

Efficiency of Attention Model. To demonstrate the efficiency of the attention model, we visualize the attention maps of different stages in Fig. 6. The discarded regions are

colored as black. Most redundant regions like “background” and “plant” are first filtered out. The important regions are then pass through the rest stages.

5 Conclusion

This paper proposed an Attention Convolutional Neural Network (ACNN) to integrate the attention mechanism into CNNs. ACNN has the ability to select informative and imperative regions. In other words, it can discard the redundant regions of the input feature maps. What’s more, it doesn’t require extra manual annotations. We trained the network in a reinforced way to learn the attentions. We also visualized the attention maps to demonstrate the efficiency of our approach. This work is a new exploration about attention mechanism in the field of human pose estimation. We achieved the state-of-the-art results on MPII human pose dataset.

References

1. Yang, Weilong, Y. Wang, and G. Mori. "Recognizing human actions from still images with latent poses." *Computer Vision and Pattern Recognition IEEE*, 2010:2030-2037.
2. Wang, Chunyu, Y. Wang, and A. L. Yuille. "An Approach to Pose-Based Action Recognition." *Computer Vision and Pattern Recognition IEEE*, 2013:915-922.
3. Yamaguchi, K, et al. "Parsing clothing in fashion photographs." *Computer Vision and Pattern Recognition IEEE*, 2012:3570-3577.
4. Yang, Wei, P. Luo, and L. Lin. "Clothing Co-parsing by Joint Image Segmentation and Labeling." *Computer Vision and Pattern Recognition IEEE*, 2014:3182 - 3189.
5. Sapp, Ben, and B. Taskar. "MODEC: Multimodal Decomposable Models for Human Pose Estimation." *IEEE Conference on Computer Vision and Pattern Recognition IEEE Computer Society*, 2013:3674-3681.
6. Felzenszwalb, Pedro, D. Mcallester, and D. Ramanan. "A discriminatively trained, multiscale, deformable part model." *Cvpr* 8:(2008):1-8.
7. Pishchulin, Leonid, et al. "Strong Appearance and Expressive Spatial Models for Human Pose Estimation." *IEEE International Conference on Computer Vision IEEE Computer Society*, 2013:3487-3494.
8. Bourdev, Lubomir D., and J. Malik. "Poselets: Body Part Detectors Trained Using 3D Human Pose Annotations." (2009):1365-1372.
9. Johnson, S, and M. Everingham. "Learning effective human pose estimation from inaccurate annotation." *Computer Vision and Pattern Recognition IEEE*, 2011:1465-1472.
10. Simonyan, Karen, and A. Zisserman. "Very Deep Convolutional Networks for Large-Scale Image Recognition." *Computer Science* (2014).
11. Szegedy, Christian, et al. "Going deeper with convolutions." *IEEE Conference on Computer Vision and Pattern Recognition IEEE Computer Society*, 2015:1-9.
12. Szegedy, Christian, et al. "Rethinking the Inception Architecture for Computer Vision." *IEEE Conference on Computer Vision and Pattern Recognition IEEE Computer Society*, 2016:2818-2826.
13. Szegedy, Christian, et al. "Inception-v4, Inception-ResNet and the Impact of Residual Connections on Learning." (2016).
14. He, Kaiming, et al. "Deep Residual Learning for Image Recognition." (2015):770-778.

15. Newell, Alejandro, K. Yang, and J. Deng. "Stacked Hourglass Networks for Human Pose Estimation." (2016):483-499.
16. Toshev, Alexander, and C. Szegedy. "DeepPose: Human Pose Estimation via Deep Neural Networks." (2013):1653-1660.
17. Fischler, M. A., and R. A. Elschlager. "The Representation and Matching of Pictorial Structures." *IEEE Transactions on Computers* C-22.1(2006):67-92.
18. Felzenszwalb, Pedro F., and D. P. Huttenlocher. *Pictorial Structures for Object Recognition*. Kluwer Academic Publishers, 2005.
19. Yang, Yi, and D. Ramanan. "Articulated pose estimation with flexible mixtures-of-parts." *Computer Vision and Pattern Recognition IEEE*, 2011:1385-1392.
20. Ren, Xiaofeng, A. C. Berg, and J. Malik. "Recovering Human Body Configurations Using Pairwise Constraints between Parts." *Tenth IEEE International Conference on Computer Vision IEEE Computer Society*, 2005:824-831.
21. Tian, Tai Peng, and S. Sclaroff. "Fast globally optimal 2D human detection with loopy graph models." *Computer Vision and Pattern Recognition IEEE*, 2010:81-88.
22. Ferrari, Vittorio, et al. *2D Human Pose Estimation in TV Shows. Statistical and Geometrical Approaches to Visual Motion Analysis*. Springer Berlin Heidelberg, 2009:128-147.
23. Tompson, Jonathan, et al. "Joint Training of a Convolutional Network and a Graphical Model for Human Pose Estimation." *Eprint Arxiv* (2014):1799-1807.
24. Wei, Shih En, et al. "Convolutional Pose Machines." (2016):4724-4732.
25. Bahdanau, Dzmitry, K. Cho, and Y. Bengio. "Neural Machine Translation by Jointly Learning to Align and Translate." *Computer Science* (2014).
26. Xu, Kelvin, et al. "Show, Attend and Tell: Neural Image Caption Generation with Visual Attention." *Computer Science* (2015):2048-2057.
27. Andriluka, Mykhaylo, et al. "2D Human Pose Estimation: New Benchmark and State of the Art Analysis." *Computer Vision and Pattern Recognition IEEE*, 2014:3686-3693.
28. Girshick, Ross. "Fast R-CNN." *Computer Science* (2015).
29. Ren, Shaoqing, et al. "Faster R-CNN: towards real-time object detection with region proposal networks." *International Conference on Neural Information Processing Systems MIT Press*, 2015:91-99.
30. Redmon, Joseph, et al. "You Only Look Once: Unified, Real-Time Object Detection." (2015):779-788.
31. Liu, Wei, et al. "SSD: Single Shot MultiBox Detector." (2015):21-37.
32. Nair, Vinod, and G. E. Hinton. "Rectified linear units improve restricted boltzmann machines." *International Conference on International Conference on Machine Learning Omnipress*, 2010:807-814.
33. Yang, Yi, and D. Ramanan. "Articulated Human Detection with Flexible Mixtures of Parts." *IEEE Trans Pattern Anal Mach Intell* 35.12(2013):2878-2890.
34. Tompson, Jonathan, et al. "Efficient object localization using Convolutional Networks." (2014):648-656.
35. Sergey Ioffe, Christian Szegedy. "Batch Normalization: Accelerating Deep Network Training by Reducing Internal Covariate Shift. *ArXiv e-prints*." (2015):448-456.
36. Pishchulin, Leonid, et al. "DeepCut: Joint Subset Partition and Labeling for Multi Person Pose Estimation." *Computer Vision and Pattern Recognition IEEE*, 2016:4929-4937.
37. Lifshitz, Ita, E. Fetaya, and S. Ullman. "Human Pose Estimation Using Deep Consensus Voting." *European Conference on Computer Vision Springer International Publishing*, 2016:246-260.

38. Gkioxari, Georgia, A. Toshev, and N. Jaitly. "Chained Predictions Using Convolutional Neural Networks." *European Conference on Computer Vision* Springer, Cham, 2016:728-743.
39. Rafi, Umer, et al. "An Efficient Convolutional Network for Human Pose Estimation." *British Machine Vision Conference 2016*:109.1-109.11.
40. Insafutdinov, Eldar, et al. "DeeperCut: A Deeper, Stronger, and Faster Multi-person Pose Estimation Model." *European Conference on Computer Vision* Springer, Cham, 2016:34-50.
41. Luvizon, Diogo C., H. Tabia, and D. Picard. "Human Pose Regression by Combining Indirect Part Detection and Contextual Information." (2017).
42. Ning, Guanghan, Z. Zhang, and Z. He. "Knowledge-Guided Deep Fractal Neural Networks for Human Pose Estimation." *IEEE Transactions on Multimedia* PP.99(2017):1-1.
43. Chu, Xiao, et al. "Multi-Context Attention for Human Pose Estimation." (2017).
44. Chou, Chia Jung, J. T. Chien, and H. T. Chen. "Self Adversarial Training for Human Pose Estimation." (2017).
45. Chen, Yu, et al. "Adversarial PoseNet: A Structure-aware Convolutional Network for Human Pose Estimation." (2017):1221-1230.
46. Yang, Wei, et al. "Learning Feature Pyramids for Human Pose Estimation." (2017):1290-1299.